Constraints on PDFs from D0

Terrence Toole for the D0 Collaboration

University of Maryland - Dept of Physics
College Park, MD 20742-4111 - U.S.A.

We present three recent results from the D0 collaboration which are sensitive to Parton Distribution Functions (PDFs). The measurements are made using data collected during Run II at the Fermilab Tevatron.

1 Introduction

There exists an interdependency between the Run II physics program at the Tevatron and PDFs. A good understanding of PDFs is critical to the success of the physics program. Most measurements at the Tevatron use PDFs as an input at some level. With a large data set in hand, the Tevatron experiments can contribute to our understanding of PDFs. Because the Tevatron is colliding $p\bar{p}$ at $\sqrt{s} = 1.96$ TeV, some of these contributions are unique to the Tevatron experiments. For the processes used, a large fraction of the events come from lower order diagrams which are theoretically well understood, and have clean signatures with low backgrounds. The D0 detector has excellent coverage for electrons and muons in both central and forward regions. This enables D0 to measure over much of the x and Q^2 range that is accessible at the Tevatron.

We present three recent D0 analyses which are sensitive to PDFs. The first is the rapidity distribution for Z bosons which uses final state electrons [2]. The W charge asymmetry is described for $W \to \mu\nu$ [3]. The last analysis is a differential cross section measurement for $\gamma+$ jet events [4].

2 Z boson rapidity

The primary source of Z production at the Tevatron is from $q\bar{q}$ annihilation. The Q^2 of the interaction is roughly the Z mass squared (M_Z^2). At leading order, the momentum fraction carried by the incident quarks is related to the boson rapidity by $x_{1,2} = \frac{M_Z}{\sqrt{s}} e^{\pm y}$ where $x_{1,2}$ is the momentum fraction carried by the incident quark and antiquark and y is the boson rapidity. As $|y|$ increases, $\Delta x = |x_1 - x_2|$ increases. At large values of $|y|$, the initial state involves a $q(\bar{q})$ with large x and a $\bar{q}(q)$ with small x. The range of momentum fraction accessible at the Tevatron is roughly $0.003 < x < 0.8$. This measurement overlaps in (x, Q^2) with Tevatron jet measurements. Because electrons are used, systematic uncertainties are different than for jet data. For example, there is no contribution from the jet energy scale.

A measurement of the normalized differential cross section is made using

$$\frac{1}{\sigma}\left(\frac{\mathrm{d}\sigma}{\mathrm{d}y}\right)_i = \frac{(\epsilon \times A)_{\mathrm{avg}}}{N^{\mathrm{obs}}_{\mathrm{total}} - N^{\mathrm{bg}}_{\mathrm{total}}} \frac{N^{\mathrm{obs}}_i - N^{\mathrm{bg}}_i}{\Delta_i \left(\epsilon \times A\right)_i},$$

where i indicates the boson rapidity bin. In the first term on the right hand side, ϵ_{avg} is the average efficiency and A_{avg} is the average acceptance for kinematic and geometric cuts. $N^{\mathrm{obs}}_{\mathrm{total}}$ ($N^{\mathrm{bg}}_{\mathrm{total}}$) is the number of candidate bosons (background events). In the second term,

ϵ_i, A_i, $N_i^{\rm obs}$, and $N_i^{\rm bg}$ are as before, but determined in each bin i. Δ_i is the bin width. Dividing by the cross section cancels some systematic uncertainties, such as the luminosity.

The measurement is made with 0.4 fb^{-1} of data. Isolated electrons are selected from the central (forward) region that have $|\eta| < 0.9$ ($1.5 < |\eta| < 3.2$) [a]. The leading (second) electron has $p_T > 25$ GeV ($p_T > 15$ GeV). The invariant mass must be within $71 < M_{ee} < 111$ GeV. Main backgrounds come from multijet or electron plus jet events where one or more jets is misidentified as an electron. The background fraction ranges from $< 1\%$ to around 5%. Main contributions to the systematic uncertainties, depending on y, are from electron efficiencies, background, and PDFs. The current measurement is statistics limited.

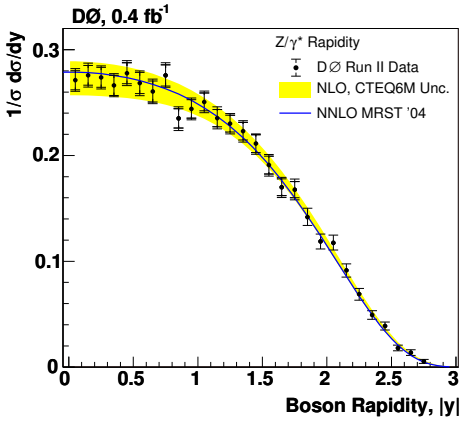

Figure 1: Z boson rapidity measured by D0. Inner (outer) error bars indicate the statistical (total) uncertainty. The spread in a NLO calculation using CTEQ6M error PDFs is shown as a yellow band. A NNLO calculation using MRST 2004 PDFs is shown as a solid line.

The result is presented in Fig. 1 as a function of $|y|$. Also shown is a NNLO curve using code from Ref. [5] and MRST 2004 PDFs [6]. The calculation is in good agreement with our data. The yellow band in Fig. 1 shows the spread when performing NLO calculations with the same code for each of the 40 CTEQ6M error PDFs [7]. At lower $|y|$ values the uncertainties are comparable to or smaller than the spread.

3 $W \to \mu\nu$ charge asymmetry

As with Z bosons, the main production mechanism for W bosons at the Tevatron is $q\bar{q}$ annihilation. A large fraction of the events involve valence-valence or valence-sea interactions. W^+ bosons are created from $u + \bar{d}$ in the initial state, with the u ($\bar{d}$) often coming from the p ($\bar{p}$). On average a u carries more momentum fraction than a d which tends to boost the $W^{+(-)}$ along the p ($\bar{p}$) direction. This produces an asymmetry in the charge separated W rapidity distribution. For leptonically decaying Ws, the ν is not measured directly, making reconstruction of y_W difficult. One approach is to measure the charge asymmetry using the μ rapidity. This contains the W charge asymmetry convoluted with the asymmetry from the (V-A) decay, which is well understood. The μ charge asymmetry is directly proportional to the $u(x)/d(x)$ ratio. The asymmetry is defined as

$$A(y_\mu) = \frac{\frac{d\sigma(\mu^+)}{dy} - \frac{d\sigma(\mu^-)}{dy}}{\frac{d\sigma(\mu^+)}{dy} + \frac{d\sigma(\mu^-)}{dy}} \quad \text{where} \quad \frac{d\sigma(\mu^\pm)}{dy} = \frac{N_i^{\mu^\pm}}{\mathcal{L} A_i \epsilon_i^\pm}.$$

Here $N_i^{\mu^\pm}$ is the number of charge separated μ candidates after background subtraction in a give rapidity bin. $\epsilon_i^\pm$ is rapidity dependent efficiency for $\mu^\pm$. $\mathcal{L}$ is the luminosity and A_i

[a] $\eta = -\ln[\tan(\theta/2)]$. In the relativistic limit $\eta = y$.

is the acceptance for μ. The acceptance and luminosity are the same for μ^+ and μ^-. They cancel in the asymmetry, which helps to minimize the measurement's dependency on PDFs.

This measurement uses 230 pb^{-1} of data. Isolated μ candidates are selected with $p_T > 20$ GeV. Candidate events are in the region $|\eta| < 2$. The events must have $\not\!\!E_T < 20$ GeV and $M_T(W) > 40$ GeV, which cut on the missing transverse energy and transverse mass respectively. Main sources of background come from electroweak processes such as $Z \to \mu\mu$ where a μ goes undetected or from $W \to \tau\mu$ where the τ decays to a μ. These backgrounds are estimated using PYTHIA [8] and are at a level of few percent. Another significant source of background comes from multijet events which can produce a μ. This contribution also is at the few percent level and is measured using data. The main contribution to the systematic uncertainty is from the efficiencies.

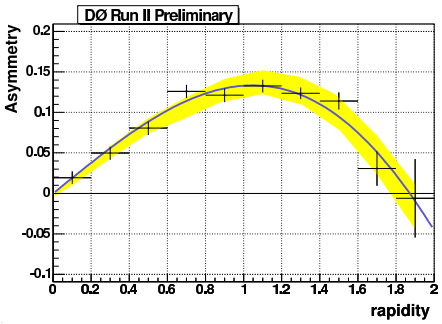

Figure 2: W charge asymmetry in the μ channel as a function of the μ | rapidity |. Error bars show the total uncertainty. In the yellow band is the spread in a NLO calculation when using CTEQ6.1M error PDFs. The solid blue curve uses the same calculation but with MRST 2002 PDFs.

The CP folded result is presented in Fig. 2. Error bars show the total uncertainty. In a yellow band is the spread obtained by following the CTEQ recipe [9] using the RESBOS-A NLO generator [10] with CTEQ6.1M 40 error PDFs. Note that in certain regions the experimental uncertainties are already smaller than the spread. Shown in a solid blue line is the RESBOS-A prediction using MRST 2002 PDF [11]. The current measurement is statistics limited.

4 Photon + jet triple differential cross section

The cross section for $p\bar{p} \to \gamma + jet + X$ is measured as a function of the p_T of the most energetic photon. The data are divided into four kinematic regions based on η^γ and η^{jet}:

Region 1: $0.0 < |\eta^\gamma| < 1.0$ and $0.0 < |\eta^{jet}| < 0.8$ and $\eta^\gamma \times \eta^{jet} > 0$
Region 2: $0.0 < |\eta^\gamma| < 1.0$ and $0.0 < |\eta^{jet}| < 0.8$ and $\eta^\gamma \times \eta^{jet} < 0$
Region 3: $0.0 < |\eta^\gamma| < 1.0$ and $1.5 < |\eta^{jet}| < 2.5$ and $\eta^\gamma \times \eta^{jet} > 0$
Region 4: $0.0 < |\eta^\gamma| < 1.0$ and $1.5 < |\eta^{jet}| < 2.5$ and $\eta^\gamma \times \eta^{jet} < 0$

Here η^{jet} is that of the leading jet. Main contributions to the "$\gamma + jet$" measurement come from the $gq \to q\gamma$ Compton diagram and from $q\bar{q}$ annihilation. The Compton diagram dominates for $p_T(\gamma) < 150$ GeV, making the measurement sensitive to the gluon distribution.

The analysis is made using 1.1 fb^{-1} of data and requires isolated photons in the central region. The leading jet must have $p_T > 15$ GeV and there is a cut on the opening angle between the photon and jet in $\eta - \phi$ space. Main backgrounds come from jet-jet or electron-jet events, where the jet or electron is misidentified as a photon. A Neural Network is used to suppress the background and also to measure the photon purity.

The main systematic uncertainty is from the luminosity (6%). After the luminosity, the main contributions to the systematic uncertainties are from the photon purity and the photon and jet selections. Each of these contributions are around 3-5%.

The result is presented in Fig. 3 along with a NLO QCD calculation using JetPhox[12] with CTEQ6.1M PDFs. Comparing data to the prediction shows some disagreement for all four regions. Similar disagreements were seen earlier by UA2 [13], CDF [14] and D0 [15]. The disagreement cannot be completely accounted for by the overall uncertainty. For more details, see Ref. [4] and O. Atramentov's report at this conference [16].

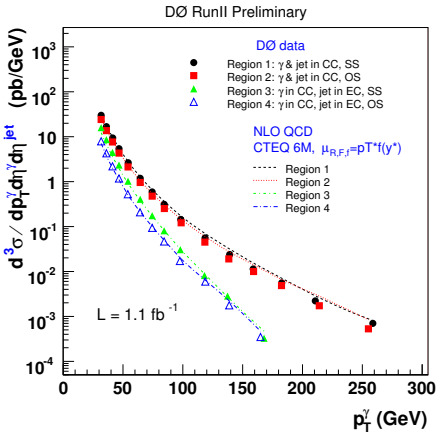

Figure 3: D0 measurement of differential cross sections for "$\gamma + jet$". Also shown are curves from NLO QCD calculation using JetPhox with CTEQ6.1M PDFs.

5 Summary

We demonstrate that even with small statistics, D0 analyses are sensitive to PDFs. We can expect significant improvements for analyses which are currently statistics limited, but are made on a small fraction of the existing data set. At the present time, D0 has more than 2.5 fb^{-1} on tape and the data set is expected to increase significantly by the end of Run II. In addition there are a number of analyses in progress, such as W, Z, or γ with a tagged b or c jet, which will complement the efforts presented here.

References

[1] `http://indico.cern.ch/contributionDisplay.py?contribId=277&sessionId=8&confId=9499`
[2] V. M. Abazov *et al.* [D0 Collaboration], arXiv:hep-ex/0702025.
[3] http://www-d0.fnal.gov/Run2Physics/WWW/results/prelim/EW/E14/E14.pdf
[4] http://www-d0.fnal.gov/Run2Physics/WWW/results/prelim/QCD/Q07/Q07.pdf
[5] C. Anastasiou *et al.*, Phys. Rev. D **69** (2004) 094008 [arXiv:hep-ph/0312266].
[6] R. S. Thorne *et al.*, arXiv:hep-ph/0407311.
[7] D. Stump *et al.*, JHEP **0310** (2003) 046 [arXiv:hep-ph/0303013].
[8] T. Sjostrand *et al.*, Comput. Phys. Commun. **135** (2001) 238 [arXiv:hep-ph/0010017].
[9] J. Pumplin *et al.*, JHEP **0207** (2002) 012 [arXiv:hep-ph/0201195].
[10] Q. H. Cao and C. P. Yuan, Phys. Rev. Lett. **93** (2004) 042001 [arXiv:hep-ph/0401026].
[11] R. S. Thorne *et al.*, Acta Phys. Polon. B **33**, 2927 (2002) [arXiv:hep-ph/0207067].
[12] P. Aurenche, R. Baier, M. Fontannaz and D. Schiff, Nucl. Phys. B **297** (1988) 661;
F. Aversa, P. Chiappetta, M. Greco and J. P. Guillet, Nucl. Phys. B **327** (1989) 105;
S. Catani, M. Fontannaz, J. P. Guillet and E. Pilon, JHEP **0205** (2002) 028 [arXiv:hep-ph/0204023].
[13] J. Alitti *et al.* [UA2 Collaboration], Phys. Lett. B **263** (1991) 544.
[14] D. Acosta *et al.* [CDF Collaboration], Phys. Rev. D **65** (2002) 112003 [arXiv:hep-ex/0201004].
[15] V. M. Abazov *et al.* [D0 Collaboration], Phys. Lett. B **639** (2006) 151 [arXiv:hep-ex/0511054].
[16] `http://indico.cern.ch/contributionDisplay.py?contribId=173&sessionId=6&confId=9499`